Available online at www.sciencedirect.com

ScienceDirect

Procedia Structural Integrity 57 (2024) 810–816

Structural Integrity Procedia

www.elsevier.com/locate/procedia

Fatigue Design 2023 (FatDes 2023)

Fatigue assessment of steel tube-to-flange welded joints with reinforcement ribs subjected to multiaxial loads according to the Peak Stress Method

Alberto Visentin[a], Alberto Campagnolo[a], Vittorio Babini[b], Giovanni Meneghetti[a]*

[a]*Department of Industrial Engineering, University of Padova, Via Venezia 1, Padova 35131, Italy*
[a]*Antonio Zamperla S.p.a, Via Monte Grappa 15/17, Altavilla Vicentina, 36007, Italy*

Abstract

In fatigue design of welded structures, the Peak Stress Method (PSM) is a FE-oriented tool to estimate the Notch Stress Intensity Factors (NSIFs). In compliance with proper fatigue design curves validated against more than 1300 experimental data, the PSM allows to estimate the fatigue lifetime of welded structures made of either aluminium alloys or structural steels and subjected to uniaxial and multiaxial loadings. Moreover, an interactive analysis tool has also been developed in Ansys® Mechanical to automate PSM application on welded structures and support the FE analyst. In this work, the fatigue strength of complex steel tube-to-flange welded joints with reinforcement ribs has been experimentally investigated under pure bending, pure torsion and in-phase as well as out-of-phase combined bending-torsion loadings. The tested joint consists of a steel SHS tube having 6.3 mm thickness, which is joined at both ends to a 15-mm-thick flange. In addition, tube and flanges are joined by fillet welding to 6-mm-thick steel reinforcement ribs. A test rig has been designed in order to perform the experimental fatigue tests, taking advantage of two hydraulic actuators. The experimental fatigue results have been compared with fatigue lifetime estimations performed using the automated PSM tool.

© 2024 The Authors. Published by Elsevier B.V.
This is an open access article under the CC BY-NC-ND license (https://creativecommons.org/licenses/by-nc-nd/4.0)
Peer-review under responsibility of the scientific committee of the Fatigue Design 2023 organizers

Keywords: welded joint; structural steel; fatigue; multiaxial loading; Peak Stress Method

* Corresponding author. Tel.: +39 049 827 67 51
E-mail address: giovanni.meneghetti@unipd.it

2452-3216 © 2024 The Authors. Published by ELSEVIER B.V.
This is an open access article under the CC BY-NC-ND license (https://creativecommons.org/licenses/by-nc-nd/4.0)
Peer-review under responsibility of the scientific committee of the Fatigue Design 2023 organizers
10.1016/j.prostr.2024.03.087

1. Introduction

Among fatigue approaches based on the Notch Stress Intensity Factors (NSIFs), which assume the weld toe and the weld root as sharp V-notches having notch tip radius $\rho = 0$ mm and notch opening angle $2\alpha = 0°$ at the weld root and $2\alpha = 135°$ at the weld toe, the Peak Stress Method (PSM) to rapidly estimate the NSIFs using coarse meshes has been coupled with the averaged Strain Energy Density (SED) fatigue criterion in (Meneghetti and Lazzarin 2011). For more details about either the PSM or the averaged SED approach the reader is referred to previous works (Lazzarin and Zambardi 2001; Livieri and Lazzarin 2005; Meneghetti and Lazzarin 2007; Lazzarin et al. 2008; Meneghetti 2012, 2013), since only the main equations and parameters will be recalled here for sake of brevity.

Dealing with arc-welded structures subjected to constant amplitude (CA) multiaxial loadings, the equivalent peak stress range has been defined by Eq. (1) as the fatigue damage parameter (Meneghetti et al. 2017a, b), which in a uniaxial plane strain state generates the same local SED existing at the weld toe or the weld root subjected to a general mixed mode I+II+III stress state.

$$\Delta\sigma_{eq,peak} = \sqrt{c_{w1} \cdot f_{w1}^2 \cdot \Delta\sigma_{\theta\theta,\theta=0,peak}^2 + c_{w2} \cdot f_{w2}^2 \cdot \Delta\tau_{r\theta,\theta=0,peak}^2 + c_{w3} \cdot f_{w3}^2 \cdot \Delta\tau_{\theta z,\theta=0,peak}^2} \tag{1}$$

In previous expression:

- $\sigma_{\theta\theta,\theta=0,peak}$, $\tau_{r\theta,\theta=0,peak}$, and $\tau_{\theta z,\theta=0,peak}$ are the opening (mode I), sliding (mode II) and tearing (mode III) peak stresses, respectively, calculated at the potential crack initiation location, i.e. the weld toe or the weld root, from linear elastic 2D or 3D FE analyses where coarse meshes are employed. It is worth noting that the PSM coupled with 3D FE models meshed with tetrahedral elements requires that the moving averages of the peak stresses are calculated on three adjacent vertex nodes, i.e. $\bar{\sigma}_{\theta\theta,\theta=0,peak}$, $\bar{\tau}_{r\theta,\theta=0,peak}$ and $\bar{\tau}_{\theta z,\theta=0,peak}$, according to Eq. (2):

$$\bar{\sigma}_{ij,\theta=0,peak,n=k} = \left. \frac{\sigma_{ij,\theta=0,peak,n=k-1} + \sigma_{ij,\theta=0,peak,n=k} + \sigma_{ij,\theta=0,,peak,n=k+1}}{3} \right|_{n=node} \quad \text{where } ij = \theta\theta, r\theta, \theta z \tag{2}$$

  The averaged peak stresses are to be input in Eq. (1) in place of the corresponding peak stresses $\sigma_{\theta\theta,\theta=0,peak}$, $\tau_{r\theta,\theta=0,peak}$, and $\tau_{\theta z,\theta=0,peak}$, respectively, as discussed in (Campagnolo et al. 2019; Meneghetti et al. 2022).

- f_{wi} ($i = 1, 2, 3$ being the local stress mode) is a parameter defined in (Meneghetti and Lazzarin 2007; Meneghetti 2012, 2013), which takes into account the coupling between the PSM and the averaged SED fatigue criterion. f_{wi} depends on the FE type and average size d, the material structural volume size R_0 and the V-notch opening angle 2α.

- c_{wi} (i = 1, 2, 3 being the local stress mode) is a parameter which accounts for the mean stress effect when the PSM is applied to stress-relieved joints. It depends on the nominal load ratio R_i and its expression has been derived in (Lazzarin et al. 2004). For as-welded joints $c_{wi} = 1$, regardless of the nominal load ratio R_i.

After having calculated the equivalent peak stress at the critical location of the welded structure through Eq. (1), the obtained value is compared with the proper reference design curve in order to estimate the fatigue life of the structure. To this aim, first, a local biaxiality ratio λ must be calculated as a function of the peak stresses according to Eq. (3):

$$\lambda = \frac{c_{w2} \cdot f_{w2}^2 \cdot \Delta\tau_{r\theta,\theta=0,peak}^2 + c_{w3} \cdot f_{w3}^2 \cdot \Delta\tau_{\theta z,\theta=0,peak}^2}{c_{w1} \cdot f_{w1}^2 \cdot \Delta\sigma_{\theta\theta,\theta=0,peak}^2} \tag{3}$$

secondly, the proper fatigue design curve is selected as a function of λ following the recommendations proposed in (Meneghetti and Campagnolo 2020) and summarized in Table 1. The recent developments of the PSM include its extension to variable amplitude (VA) multiaxial loadings (Campagnolo et al. 2022) and the development of an interactive analysis tool in Ansys® Mechanical to support the FE analyst in automating the fatigue design of complex welded structures (Visentin et al. 2022).

Table 1. Criterion for selecting the reference PSM-based fatigue design curve for steel arc-welded joints (Meneghetti and Campagnolo 2020)

λ Eq. (3)	N_A [cycles]	$\Delta\sigma_{eq,peak,A,50\%}$ [MPa]	$\Delta\sigma_{eq,peak,A,97.7\%}$ [MPa]	$\Delta\sigma_{eq,peak,A,2.3\%}$ [MPa]	k* [-]	T_σ** [-]
$\lambda = 0$	$2\cdot10^6$	214	156	296	3	1.90
$\lambda > 0$	$2\cdot10^6$	354	257	488	5	1.90

* k = inverse slope (see Fig. 6); ** T_σ = scatter index (2.3% - 97.7%) (see Fig. 6).

2. Joint geometry and experimental fatigue tests

The fatigue strength of S355 steel tube-to-flange arc-welded joints with reinforcement ribs (Fig. 1) has been experimentally investigated under pure bending, pure torsion and in-phase as well as out-of-phase combined bending-torsion loadings. The tested joint consists of a steel SHS 80x80 mm tube having 6.3 mm thickness, which is joined at both ends to a 15-mm-thick flange. In addition, tube and flanges are joined by fillet welding to 6-mm-thick steel reinforcement ribs. A test rig has been designed in order to perform the experimental fatigue tests, (Fig. 2). One specimen's flange is bolted to a vertical support, the other one being bolted to a lever arm, which is loaded at its extremities by means of two servo-hydraulic actuators equipped with 15 kN load cells. The specimen's flange at the lever arm side has a threaded central hole, where a tube delivering pressurized air at 0.8 MPa is connected. To allow for the arc-shaped trajectory of the lever arm extremities caused by the torsional rotation, a connecting rod was employed between each servo-hydraulic cylinder and the lever arm, as shown in Fig. 2.

The external loads F_1 and F_2 exerted by the hydraulic actuators according to Fig. 2 resulted in bending and torsion moments at the weld toe of the reinforcement rib as follows:

$$M_b(t) = [F_1(t) + F_2(t)] \cdot b \tag{4a}$$

$$M_t(t) = [F_1(t) - F_2(t)] \cdot i \tag{4b}$$

where b and i are the bending and torsion moment arms, respectively. The nominal bending and torsion stresses at the weld toe of the reinforcement rib can be expressed as:

$$\sigma(t) = \frac{M_b(t)}{W_b} = \frac{\Delta\sigma}{2}\sin(2\pi ft) + \sigma_m \qquad \tau(t) = \frac{M_t(t)}{W_t} = \frac{\Delta\tau}{2}\sin(2\pi ft + \varphi) + \tau_m \tag{5}$$

W_b and W_t being the section moduli. By taking advantage of Eqs. (4) and (5), the external loads F_1 and F_2 to apply can be derived as functions of the desired values of: (i) the nominal bending and torsion stress ranges at the weld toe of the reinforcement rib, $\Delta\sigma$ and $\Delta\tau$, respectively, (ii) the mean values, σ_m and τ_m, and (iii) the phase shift φ. The reader is referred to (Frendo and Bertini 2015) for the general expressions of the external loads, which are not reported here for sake of brevity.

Tests were carried out under constant amplitude pulsating ($R = 0.1$) fatigue loadings. In the case of bending-torsion tests, both in-phase ($\varphi = 0$) as well as out-of-phase ($\varphi = 90°$) nominal stresses with nominal biaxiality ratios $\Lambda = \tau/\sigma = 1$ and $\Lambda = \tau/\sigma = 1/\sqrt{3}$ have been applied. All fatigue tests were run under closed-loop load control by using an MTS FlexTest® GT60 digital controller in standard laboratory environment. To determine the number of cycles to break-through, the specimen's flange at the lever arm side was connected to a pneumatic circuit operating at about 0.8 MPa, see Fig. 2. A sudden pressure drop in the tube occurs when a through-the-thickness crack occurs. The number of cycles to break-through (N_{bt}) was determined when a 2% pressure drop was detected by the pressure switch, with respect to the initial pressure. The number of cycles to break-through was assumed as failure criterion.

All specimens were tested in as-welded conditions. Fatigue crack initiation always occurred at the weld toe between the tube and the reinforcement ribs (Fig. 3). Fig. 5 reports the number of cycles to break-through as a function of the Von Mises equivalent stress range $\Delta\sigma_{VM} = \sqrt{\Delta\sigma^2 + 3\cdot\Delta\tau^2}$ calculated at the weld toe of the reinforcement ribs for all fatigue tests. It should be noted that, first, the nominal stress range has been calculated separately for each stress component, i.e. $\Delta\sigma$ and $\Delta\tau$. After that, they have been used to compute the Von Mises equivalent stress range.

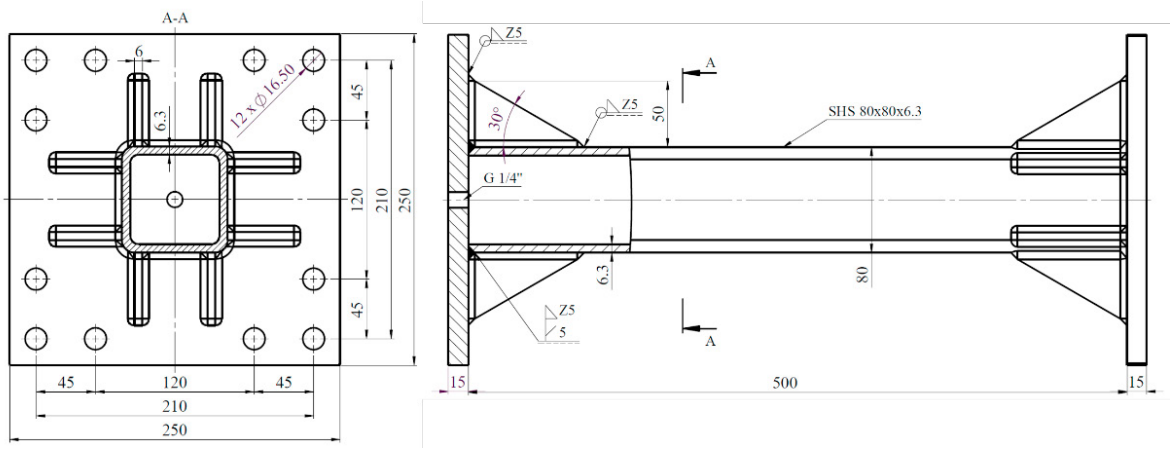

Figure 1. Tube-to-flange steel welded joints with reinforcement ribs. Dimensions of the tested specimens (in millimeters).

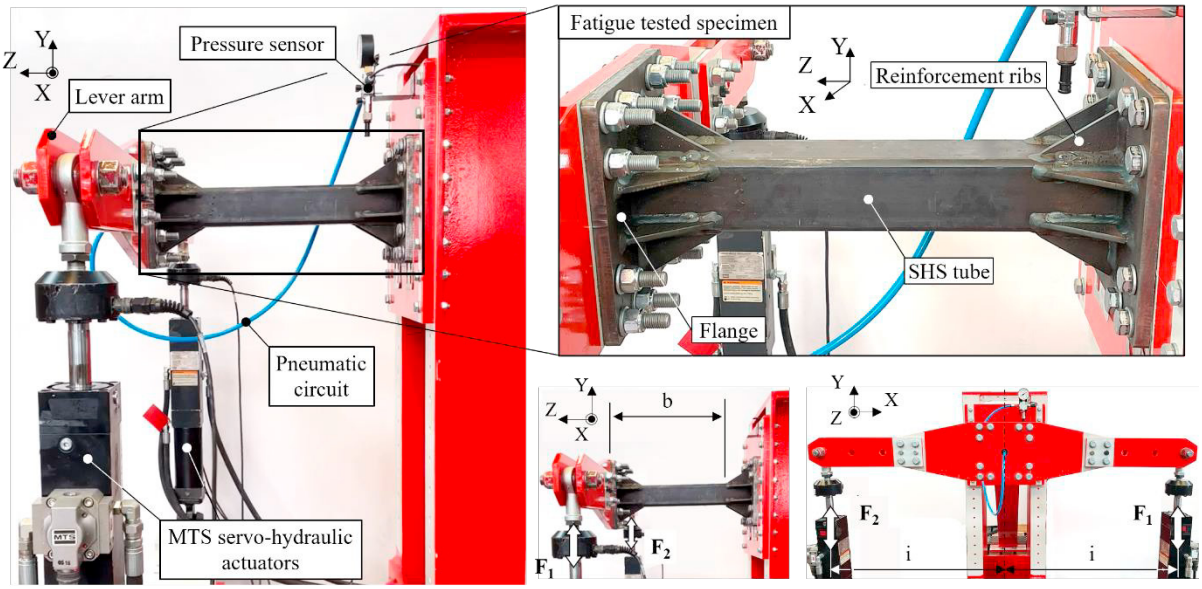

Figure 2. Test rig adopted to perform pure bending, pure torsion and combined bending and torsion fatigue tests on tube-to-flange steel welded joints with reinforcement ribs.

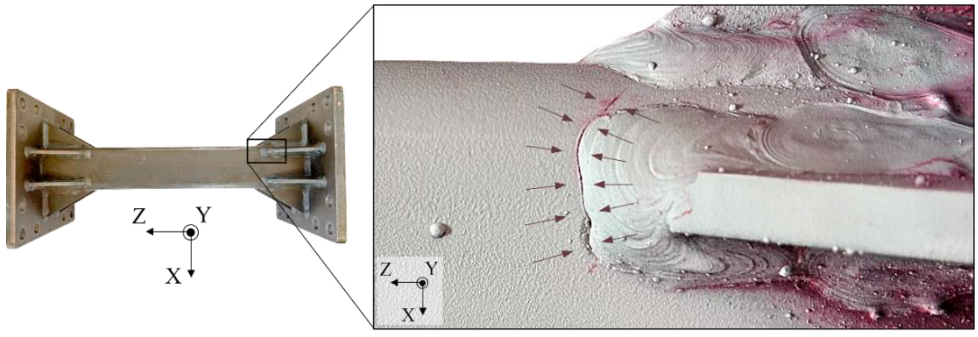

Figure 3. Fatigue crack path analysed by means of dye penetrant inspection: through-the-thickness fatigue crack initiated and propagated at the weld toe between the tube and a reinforcement rib in a specimen fatigue tested under out-of-phase ($\varphi = 90°$) bending-torsion constant amplitude loading.

3. Fatigue strength assessment according to the PSM

A finite element (FE) model of the joint under exam has been generated in Ansys® Mechanical by exploiting a quarter of the entire geometry due to the symmetry with respect to XZ and YZ planes and a 10-node tetrahedral FE mesh. The profile of the weld toes between the tube and the reinforcement ribs has been modelled by approximating the real geometry of the weld beads (Fig. 4). Loads and constraints have been applied to the FE model in order simulate pure bending, pure torsion and combined bending and torsion loadings (Fig. 4). Owing to the possibility to employ a dedicated tool that enables full-automated application of the PSM in Ansys® Mechanical (see (Visentin et al. 2022)), all weld toes of the model have been investigated in order to identify the fatigue crack initiation points and assess the fatigue strength of the welded connections between the tube and the reinforcement ribs. In order to grant PSM applicability at weld toes and account for mode I and mode III loadings, a mesh density ratio $a/d \geq 3$ must be guaranteed, according to (Meneghetti and Campagnolo 2020). The notch characteristic size a equals the minimum value between the thickness of the ribs, i.e. 6 mm, and the thickness of the tube, i.e. 6.3 mm (Fig. 1). Accordingly, a 10-node tetrahedral mesh having global element size $d = 6.0/3 = 2.0$ mm has been generated over the model (Fig. 4).

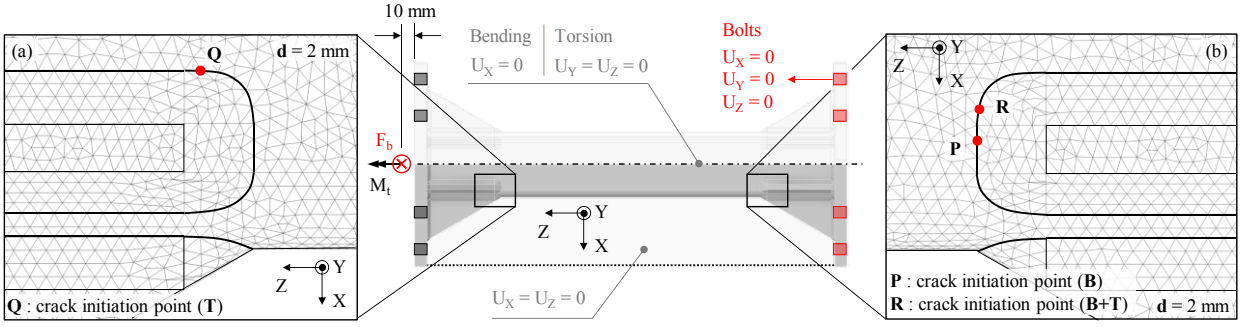

Figure 4. FE analyses performed in Ansys® Mechanical to assess the fatigue strength of tube-to-flange steel welded joints with reinforcement ribs under pure bending, pure torsion and combined bending and torsion loadings. (a) Detail of the FE mesh (lever arm side) and identified crack initiation point 'Q' in the case of pure torsion (T) loading. (b) Detail of the FE mesh (support side) and identified crack initiation points 'P' and 'R' in the case of pure bending (B) and combined bending and torsion (B+T) loadings respectively.

In the case of pure torsion loading, the PSM identified node 'Q' (Fig. 4a) as fatigue crack initiation point at the weld toe between the tube and the reinforcement ribs on the lever arm side. In the case of pure bending and combined bending and torsion loadings, the PSM identified nodes 'P' and 'R' (Fig. 4b) as fatigue crack initiation points along the weld toe between the tube and the reinforcement ribs on the support side, in compliance with experimental observations (Fig. 3). The local biaxiality ratio λ evaluated according to Eq. (3) at the relevant estimated crack initiation point resulted equal to zero in the case of pure bending loading, while it was greater than zero in the case of pure torsion and combined bending and torsion loadings. Eventually, a good agreement can be observed between the experimental fatigue data, expressed in terms of the equivalent peak stress, and the proposed PSM-based fatigue design scatter bands for $\lambda = 0$ (Fig. 6a) and $\lambda > 0$ (Fig. 6b).

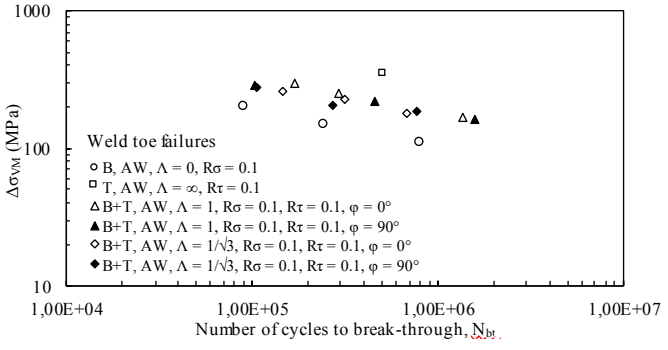

Figure 5. Experimental fatigue data of tube-to-flange welded joints with reinforcement ribs evaluated in terms of the Von Mises equivalent stress.

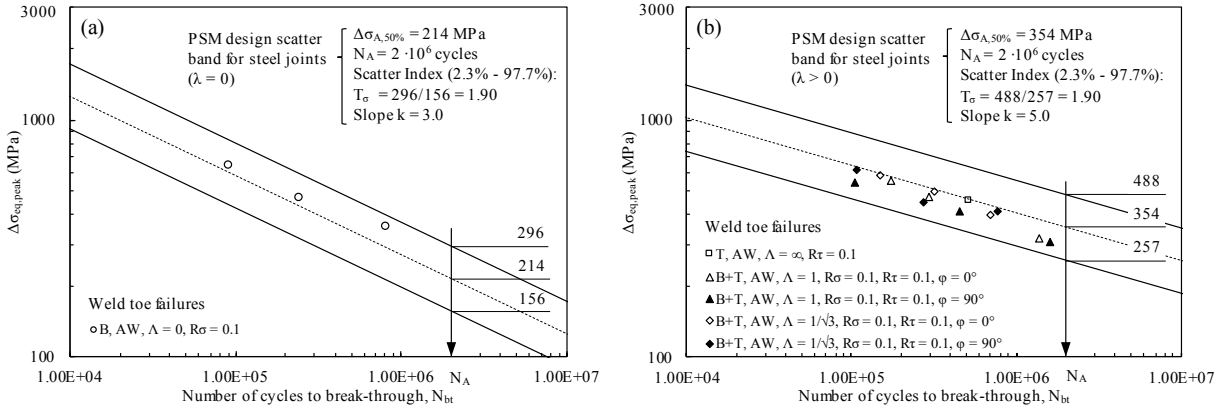

Figure 6. Fatigue assessment of tube-to-flange welded joints with reinforcement ribs according to the PSM. (a) Comparison between the PSM-based fatigue design scatter band ($\lambda = 0$) and the experimental fatigue data evaluated in terms of the equivalent peak stress. (b) Comparison between the PSM-based fatigue design scatter band ($\lambda > 0$) and the experimental fatigue data evaluated in terms of the equivalent peak stress. The design scatter bands were calibrated in Refs. (Meneghetti and Lazzarin 2011; Meneghetti 2013), respectively, and are not fitted on the experimental data shown in the figure.

4. Conclusions

In this work, the fatigue strength of tube-to-flange S355 steel arc-welded joints with reinforcement ribs under constant amplitude multiaxial loading has been investigated. A test rig has been designed to fatigue test the specimens under pure bending, pure torsion as well as combined bending and torsion constant amplitude loadings. All tested specimens exhibited crack initiation and propagation at the weld toe between the tube and the reinforcement ribs. The developed PSM tool has been adopted to automatically assess the fatigue strength of the welded details according to the PSM. The PSM correctly identified the fatigue crack initiation point, i.e. the weld toe between the tube and the reinforcement ribs, in all considered load cases. Moreover, a good agreement has been obtained between the experimental fatigue data, evaluated in terms of the equivalent peak stress, and the proposed PSM-based fatigue design scatter bands for steel joints. Additional constant amplitude as well as variable amplitude pure bending, pure torsion and combined bending and torsion fatigue tests are currently planned. Eventually, fatigue cracks initiation and propagation in broken specimens will be the subject of more detailed future investigation.

References

Amstutz H, Storzel K, Seeger T (2001) Fatigue crack growth of a welded tube-flange connection under bending and torsional loading. Fatigue Fract Eng Mater Struct 24:357–368. https://doi.org/10.1046/j.1460-2695.2001.00408.x

Campagnolo A, Roveda I, Meneghetti G (2019) The Peak Stress Method combined with 3D finite element models to assess the fatigue strength of complex welded structures. Procedia Struct Integr 19:617–626. https://doi.org/10.1016/j.prostr.2019.12.067

Campagnolo A, Vecchiato L, Meneghetti G (2022) Multiaxial variable amplitude fatigue strength assessment of steel welded joints using the peak stress method. Int J Fatigue 163:107089. https://doi.org/10.1016/j.ijfatigue.2022.107089

Frendo F, Bertini L (2015) Fatigue resistance of pipe-to-plate welded joint under in-phase and out-of-phase combined bending and torsion. Int J Fatigue 79:46–53. https://doi.org/10.1016/j.ijfatigue.2015.04.020

Lazzarin P, Livieri P, Berto F, Zappalorto M (2008) Local strain energy density and fatigue strength of welded joints under uniaxial and multiaxial loading. Eng Fract Mech 75:1875–1889. https://doi.org/10.1016/j.engfracmech.2006.10.019

Lazzarin P, Sonsino CM, Zambardi R (2004) A notch stress intensity approach to assess the multiaxial fatigue strength of welded tube-to-flange joints subjected to combined loadings. Fatigue Fract Eng Mater Struct 27:127–140. https://doi.org/10.1111/j.1460-2695.2004.00733.x

Lazzarin P, Zambardi R (2001) A finite-volume-energy based approach to predict the static and fatigue behavior of components with sharp V-shaped notches. Int J Fract 112:275–298. https://doi.org/10.1023/A:1013595930617

Livieri P, Lazzarin P (2005) Fatigue strength of steel and aluminium welded joints based on generalised stress intensity factors and local strain energy values. Int J Fract 133:247–276. https://doi.org/10.1007/s10704-005-4043-3

Meneghetti G (2012) The use of peak stresses for fatigue strength assessments of welded lap joints and cover plates with toe and root failures. Eng Fract Mech 89:40–51. https://doi.org/10.1016/j.engfracmech.2012.04.007

Meneghetti G (2013) The peak stress method for fatigue strength assessment of tube-to-flange welded joints under torsion loading. Weld World 57:265–275. https://doi.org/10.1007/s40194-013-0022-x

Meneghetti G, Campagnolo A (2020) State-of-the-art review of peak stress method for fatigue strength assessment of welded joints. Int J Fatigue 139:105705. https://doi.org/10.1016/j.ijfatigue.2020.105705
Meneghetti G, Campagnolo A, Rigon D (2017a) Multiaxial fatigue strength assessment of welded joints using the Peak Stress Method – Part I: Approach and application to aluminium joints. Int J Fatigue 101:328–342. https://doi.org/10.1016/j.ijfatigue.2017.03.038
Meneghetti G, Campagnolo A, Rigon D (2017b) Multiaxial fatigue strength assessment of welded joints using the Peak Stress Method – Part II: Application to structural steel joints. Int J Fatigue 101:343–362. https://doi.org/10.1016/j.ijfatigue.2017.03.039
Meneghetti G, Campagnolo A, Visentin A, et al (2022) Rapid evaluation of notch stress intensity factors using the peak stress method with 3D tetrahedral finite element models: Comparison of commercial codes. Fatigue Fract Eng Mater Struct. https://doi.org/10.1111/ffe.13645
Meneghetti G, Lazzarin P (2011) The Peak Stress Method for Fatigue Strength Assessment of welded joints with weld toe or weld root failures. Weld World 55:22–29. https://doi.org/10.1007/BF03321304
Meneghetti G, Lazzarin P (2007) Significance of the elastic peak stress evaluated by FE analyses at the point of singularity of sharp V-notched components. Fatigue Fract Eng Mater Struct 30:95–106. https://doi.org/10.1111/j.1460-2695.2006.01084.x
Razmjoo GR (1996) Fatigue of load carrying fillet welded joints under multiaxial loading. Fatigue core research from TWI. Abington Publishing, Abington
Sonsino CM (1997) Fatigue strength of welded components under complex elasto-plastic, multiaxial deformations
Visentin A, Campagnolo A, Babini V, Meneghetti G (2022) Automated implementation of the Peak Stress Method for the fatigue assessment of complex welded structures. Forces Mech 100072. https://doi.org/10.1016/j.finmec.2022.100072
Yousefi F, Witt M, Zenner H (2001) Fatigue strength of welded joints under multiaxial loading: experiments and calculations. Fatigue Fract Eng Mater Struct 24:339–355. https://doi.org/10.1046/j.1460-2695.2001.00397.x